Applied Mathematics and Computation 318 (2018) 80–91

Contents lists available at ScienceDirect

Applied Mathematics and Computation

journal homepage: www.elsevier.com/locate/amc

Separatrix reconstruction to identify tipping points in an eco-epidemiological model

Elisa Francomano[a], Frank M. Hilker[b], Marta Paliaga[a,*], Ezio Venturino[c]

[a] Scuola Politecnica, Department of Industrial and Digital Innovation, University of Palermo, Italy
[b] Institute of Environmental Systems Research, School of Mathematics/Computer Science, Osnabrück University, Germany
[c] Department of Mathematics "Giuseppe Peano", University of Torino, Italy

ARTICLE INFO

Article history:
Available online 29 July 2017

Keywords:
Dynamical system
Allee threshold
Group hunting
Radial basis function
Moving Least Squares approximation
Regime shift

ABSTRACT

Many ecological systems exhibit tipping points such that they suddenly shift from one state to another. These shifts can be devastating from an ecological point of view, and additionally have severe implications for the socio-economic system. They can be caused by overcritical perturbations of the state variables such as external shocks, disease emergence, or species removal. It is therefore important to be able to quantify the tipping points. Here we present a study of the tipping points by considering the basins of attraction of the stable equilibrium points. We address the question of finding the tipping points that lie on the separatrix surface, which partitions the space of system trajectories. We present an algorithm that reconstructs the separatrix by using a Moving Least Squares approximant based on radial basis functions. The algorithm is applied to an eco-epidemiological model of pack hunting predators that suffer disease infection. Our analysis reveals that strong hunting cooperation considerably promotes the survival of predators and renders the predators resilient to perturbations.

1. Introduction

Many ecosystems can be found in one of several possible alternative stable states [6,25,27,28,33,36,38]. Consequently, such ecosystems can shift abruptly from one state to another—a phenomenon also known as ecological regime shift. Well-known examples include shifts from clear to turbid waters [10], from grassland to shrubland [34], the collapse of fisheries [32], and the degradation of coral reefs [30]. As regime shifts often imply catastrophic consequences for the ecosystem, failure to recognize alternative stable states or wrong predictions of the threshold points between them can turn out not only as a surprise, but also costly.

Regime shifts can be triggered by perturbations of the state variables or by changing parameters [6,29,35]. In the latter case, environmental drivers typically lead to the appearance (or disappearance) of alternative stable states and thus cause sudden shifts. In the former case, the ecosystem is already multistable, and an overcritical disturbance of the state variables shifts the system from the basin of attraction of one stable state to the basin of attraction of another stable state. The basins of attraction are separated by a separatrix, which corresponds to threshold values of the state variables, also called tipping points.

* Corresponding author.
E-mail addresses: elisa.francomano@unipa.it (E. Francomano), frank.hilker@uni-osnabrueck.de (F.M. Hilker), marta.paliaga@unipa.it (M. Paliaga), ezio.venturino@unito.it (E. Venturino).

http://dx.doi.org/10.1016/j.amc.2017.07.022
0096-3003/

In a simple system with one state variable only, the tipping point corresponds to the unstable equilibrium that separates two stable steady states. However, in higher dimensional systems, information about the separatrix is needed. In particular, the tipping point of a certain state variable is not a single value for a given set of parameters anymore, but it depends on the values of the other state variables as the separatrix is a higher dimensional object.

Knowledge of the existence and location of tipping points is fundamental for understanding and managing ecosystems [9,10,23,36]. Yet, theoretical ecology rarely addresses the identification of tipping points in higher dimensional systems. There is a need of methods that help in accomplishing this task. In this paper, we provide a numerical tool to locate the tipping points of a higher dimensional system. The idea is to approximate the surface that partitions state space into the two different domains of attraction, i.e. the separatrix. In [11–13] the authors divide the points in the state space into different regions depending on where the trajectories stabilize. We propose an algorithm that is able to find the points of the separatrix by limiting the search area, and we propose an alternative method to reconstruct the separatrix surface using a Moving Least Squares approximant [18,26]. This quasi-interpolant is formulated by means of radial basis functions with compact support, providing a local approximation of each evaluation point. This method, using the explicit formula of the Lagrange multipliers, avoids the setting up of a large interpolation system, thus reducing the computational cost.

We apply our method to find the tipping points of an eco-epidemiological model proposed in [24]. This model combines disease transmission in a predator population with the ecological dynamics of a predator–prey system. The feature of this model is that predators cooperate by hunting in packs. This cooperation can induce a tipping point in the predator density: if predator density is too small, the predator population goes extinct as they are not sustained by the prey. However, if the predator density is large enough, hunting cooperation mediates predator survival due to increased prey consumption. The critical predator density needed for survival corresponds to the tipping point between extinction and persistence. In ecology, this tipping point is also known as extinction threshold or as Allee threshold [7,8,15]. The Allee effect describes the positive correlation between population density and population fitness (measured as the per-capita growth rate) [3,15]. There are two types of Allee effects. Strong Allee effects are characterized by a critical threshold below which populations go extinct, whereas weak Allee effects do not induce a threshold such that small populations can survive. We will use our method to study how the Allee threshold changes for varying ecological and epidemiological parameters. We will find that the strong Allee effect can turn effectively into something similar to a weak Allee effect, of which we become aware only because we approximate the Allee threshold.

In the next Section, we introduce the eco-epidemiological model and summarize the main results on its dynamical behavior. In Section 3 we explain the algorithm developed to reconstruct the separatrix manifold, and in Section 4 we apply the algorithm to the eco-epidemiological model. The final section presents conclusions and some ideas for future work.

2. Eco-epidemiological model

In this section, we recap an eco-epidemiological model introduced and analyzed in [24]. This model exhibits bistability and will be used to illustrate the numerical tool to approximate separatrix surfaces later on.

In many biological systems animals exhibit social behavior. Pack-hunting animals are an example, where predators hunt their prey by working together with other members of their species. For example, African wild dogs [16,17] organize themselves in a coordinated formation to surround and attack their prey. Lions hunt in pack of three to seven individuals, splitting into center and wings, to ambush prey [37]. Cooperation in a group represents a mechanism developed through evolution to improve the skills of hunting and the chance of survival.

In the last decades, biomathematics has paid increasing attention to social behavior as it is well known to induce strong Allee effects. Thus, there is the possibility of extinction if population density falls below the critical value known as Allee threshold [5,15,22,24,39]. Therefore it is important to study this quantity in order to protect endangered species (or to guide eradication campaigns of pest species). Population dynamics can be modeled mathematically by means of a system of differential equations with the population densities over time as unknowns and with suitable parameters to describe population interactions such as predation. The mathematical approach coupled with experimental investigations allows to convert the underlying mechanism into a predictive science [31].

The eco-epidemiological model considered here is based on prey and predator populations with densities N and P, respectively. Predators are assumed to be cooperative hunters and to suffer an infectious disease, which is why the predator population is split into susceptibles (S) and infecteds (I), with $P = S + I$. The population dynamics in time T can be described by a three-dimensional system of nonlinear ordinary differential equations:

$$\begin{aligned}
\frac{dN}{dT} &= r\left(1 - \frac{N}{K}\right)N - (a_0 + a_1 P)NP,\\
\frac{dS}{dT} &= -\beta\frac{SI}{P} - mS + \epsilon(a_0 + a_1 P)NS + (1-\theta)\epsilon(a_0 + a_1 P)NI,\\
\frac{dI}{dT} &= \beta\frac{SI}{P} - mI - \mu I + \theta\epsilon(a_0 + a_1 P)NI.
\end{aligned}$$

We assume logistic growth in prey, with r being the per capita net growth rate and K the carrying capacity. Predators have a natural per capita death rate m and grow by consuming prey. Their functional response to prey is given by the term

Table 1
Equilibria of model (1)–(3) and their existence and stability conditions.

Equilibrium	Coordinates	Meaning
E_0	(0, 0, 0)	Extinction of all species
E_n	(k, 0, 0)	Prey only
E_i	(0, 0, 1)	Extinction of all species
E_{ni}	$(k, 0, 1-\frac{(1-\theta)k}{\beta-\mu})$	Disease-induced predator extinction
E_{np}	(n^*, p^*, 0)	Disease-free predator–prey coexistence
E_{npi}	$(n^*, p^*, \frac{\beta-\mu-(1-\theta)}{(\beta-\mu\theta)})$	(Endemic) coexistence

$(a_0 + a_1 P)N$, where a_0 is the density-independent predation rate corresponding to a linear functional response and a_1 represents the strength of hunting cooperation. Parameter ϵ is the conversion efficiency from prey to predator density. Disease transmission in the predator population is frequency-dependent, with β being the transmission parameter. Moreover, we consider the possibility of vertical transmission, i.e. the disease can be passed from mother to offspring, and $\theta \in [0, 1]$ is the fraction of offsprings acquiring infection from their mothers. Infected predators are subject to an additional disease-induced per capita death rate, μ.

To analyze the system we first replace the state variables S and I by the entire predator population $P = S + I$ and its prevalence $i = I/P$. We then nondimensionalize the system by introducing the dimensionless quantities

$$n = \frac{\epsilon a_0}{m} N, \quad p = \frac{a_0}{m} P, \quad t = mT.$$

This leads to:

$$\frac{dn}{dt} = r'\left(1 - \frac{n}{k'}\right)n - (1 + \alpha p)np, \tag{1}$$

$$\frac{dp}{dt} = -\left(1 + \mu' i\right)p + (1 + \alpha p)np, \tag{2}$$

$$\frac{di}{dt} = i(1 - i)\left(\beta' - \mu'\right) - (1 + \alpha p)(1 - \theta)ni, \tag{3}$$

where

$$r' = \frac{r}{m}, \quad k' = \frac{\epsilon a_0 K}{m}, \quad \alpha = \frac{m a_1}{a_0^2}, \quad \mu' = \frac{\mu}{m}, \quad \beta' = \frac{\beta}{m}$$

are dimensionless parameters. In particular, α represents the strength of predator cooperation and shall be of special interest along with the disease transmissibility. From now on, we drop the dashes appearing in the parameters to simplify notation.

The main goal of analyzing the model is to study the long-term behavior of the trajectories in time. Therefore, the first step is to find the equilibria of the system, i.e. the constant solutions. These points are stable if there exists a set, called the basin of attraction, that contains all the initial conditions evolving toward the equilibrium.

Solving for the equilibria of model (1)–(3), we find the ones listed in Table 1. For existence and stability conditions, please see [24].

An important quantity in the stability analysis is the basic reproduction number of the disease in the predator population,

$$R_0 = \frac{\beta}{\mu + (1 - \theta)k}, \tag{4}$$

which gives the number of secondary infections caused by a single infected predator during its lifetime when the predator–prey system is at disease-free coexistence equilibrium. We can distinguish two cases. First, if $R_0 < 1$, the infection will die out in the long run. In this case, the model reduces to the disease-free predator–prey system with predator cooperation considered in [39]. Second, if $R_0 > 1$, the disease will spread in the predator population; in this case, there may be coexistence of predators, prey, and disease or disease-induced predator extinction. To investigate the impact of pack hunting we study the bifurcation behavior by numerically continuing the equilibria and their stability as functions of the hunting cooperation parameter α. In particular, here we compare the case in which the disease cannot establish ($R_0 < 1$; left panels of Fig. 1) with the endemic case ($R_0 > 1$; right panels of Fig. 1).

In each case, we assume a baseline scenario in which predators go extinct if hunting cooperation is absent or small ($\alpha < \alpha_c$; Fig. 1C and D). In this parameter range ($\alpha < \alpha_c$) the hunting cooperation is not sufficient to avoid predator extinction. As a consequence, the prey population reaches carrying capacity (Fig. 1A and B). The system is equivalent to the classical Lotka–Volterra model with prey self-regulation in a parameter range where the prey-only equilibrium (E_n or E_{ni}) is the only attractor.

If $\alpha = \alpha_c$ a limit point occurs and there is a saddle–node bifurcation such that for $\alpha > \alpha_c$ there are two branches of nontrivial equilibria, one being stable and the other one being unstable. That is, for sufficiently large hunting cooperation

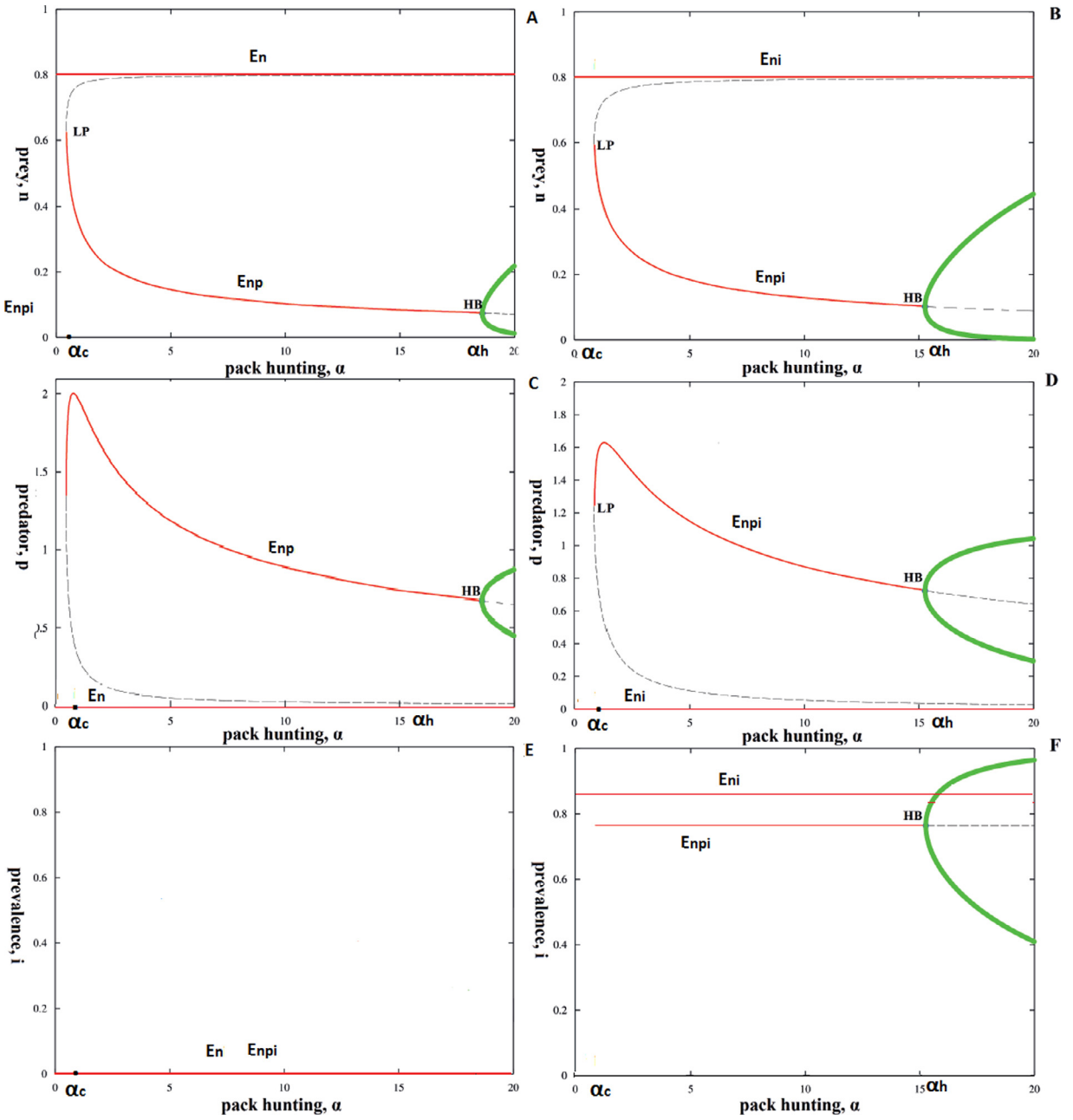

Fig. 1. Bifurcation diagrams of model (1)–(3) for varying hunting cooperation. The left panels are the disease-free case ($\beta = 0.7; R_0 < 1$) and the right panels are the endemic case ($\beta = 5; R_0 > 1$). Red lines indicate stable equilibria and dashed black lines unstable equilibria. LP marks limit point bifurcations occurring at $\alpha = \alpha_c$ and HB marks Hopf bifurcations at $\alpha = \alpha_h$. The bold green lines are the amplitudes of limit cycles. Other parameter values: $r = 10$, $k = 0.8$, $\theta = 0.1$, $m = 0.3$. (For interpretation of the references to color in this figure legend, the reader is referred to the web version of this article.)

the system is bistable. Predators either go extinct (E_n or E_{ni}) or coexist with the prey (E_{np} or E_{npi}), depending on the initial population densities. Pack hunting can thus mediate the survival of predators, in particular if the prey density cannot sustain predators in the absence of hunting cooperation. This is an emerging property not present in the classical Lotka–Volterra model.

In this parameter range, cooperation induces a strong Allee effect in the predator population. The Allee threshold is the predator density, below which predator populations go extinct, and above which they survive. It is important to note that this Allee threshold for the predator density depends on the prey population density and also on the prevalence of infection. This cannot be seen in the bifurcation diagrams. The panels in Fig. 1C and D show predator curves of the unstable coexistence state, but because we are dealing with a higher-dimensional system they do not correspond to the Allee threshold.

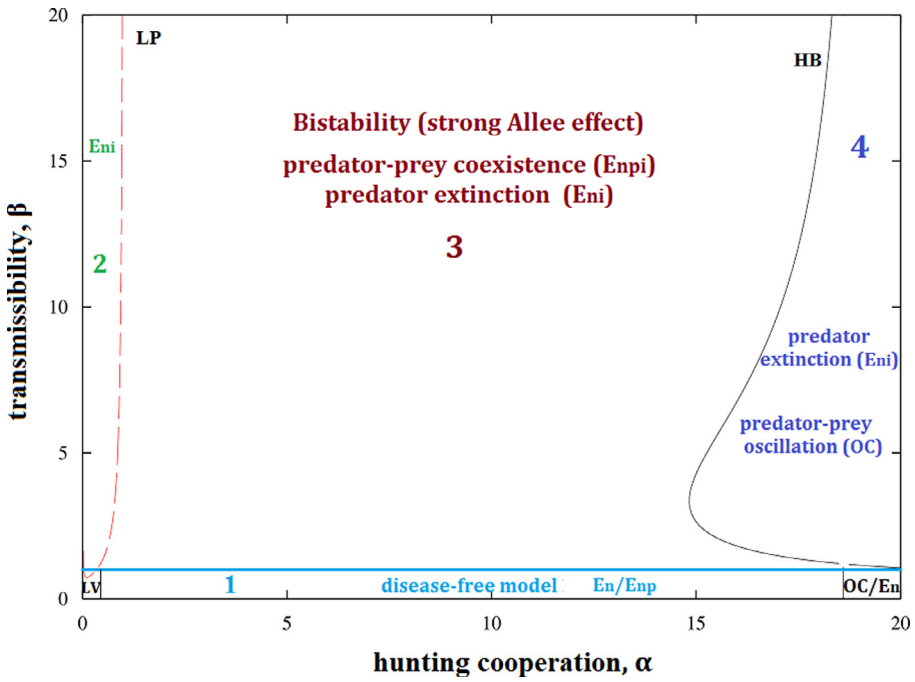

Fig. 2. Two-parameter bifurcation diagram of model (1)–(3) when varying predator cooperation α and disease transmissibility β. The red dashed line represents the limit point bifurcation curve (LP) and the black one the Hopf bifurcation curve (HB). There are four different scenarios in the endemic case: (1) disease-free model, (2) extinction of predators, (3) bistability between predator extinction and stable endemic coexistence, and (4) bistability between predator extinction of oscillatory endemic coexistence (OC). In the disease-free case, LV stands for the prey-only state of the Lotka–Volterra model with logistic prey growth. Other parameter values as in Fig. 1. (For interpretation of the references to color in this figure legend, the reader is referred to the web version of this article.)

Instead, we have to find the separatrix between the prey-only state and the coexistence state—which will be the topic of the next section.

In the remainder of this section, we complete the description of the bifurcation behavior in the eco-epidemiological model. If $\alpha > \alpha_c$ and hunting cooperation increases, the prey population density at stable coexistence equilibrium decreases because cooperating predators become more effective in exploiting the prey. In turn, predator density increases initially with increasing cooperation, but declines for larger values of α when the prey becomes overexploited.

Furthermore, for high values of predator cooperation, there is a Hopf bifurcation, where the coexistence equilibrium becomes unstable and populations start to oscillate (at $\alpha = \alpha_h$ in the bifurcation diagrams). Meanwhile the prey-only equilibrium remains stable, i.e. we continue to have bistability.

The bifurcation behavior described so far is the same for the disease-free and the endemic case. We now highlight some important differences. In the disease-free case, infection prevalence always vanishes (Fig. 1E). By contrast, when $R_0 > 1$ the prevalence can reach two different levels, depending on whether or not predators survive. (Note that if predators go extinct the prevalence is the ratio of predators infected in the limit process of the predator population density approaching zero.) These prevalence levels are independent of α (Fig. 1F and Table 1).

Probably more importantly, the disease tends to reduce the impact of hunting cooperation. Comparing the bifurcation diagrams of predators and prey for the disease-free case on the one hand and for the endemic case on the other hand we observe that the limit point occurs for larger values of α in the presence of the disease. This makes sense as due to infection there is a higher mortality rate in the predator population. This requires higher hunting cooperation to mediate predator survival, and it also reduces the peak density of predators (compare Fig. 1D with Fig. 1C).

In order to provide a more complete overview, we show a two-parameter bifurcation diagram in Fig. 2 (see also [20]). We can distinguish four different dynamical regimes:

1. For low values of β ($R_0 < 1$) the disease is not endemic. In this disease-free case, there are three different scenarios depending on the level of hunting cooperation. First, for small values of α, pack hunting is too weak to overcome predator extinction, basically corresponding to the prey-only state in the Lotka–Volterra model with prey self-regulation. Second, for higher hunting cooperation, there is bistability between the prey-only state E_n and the predator–prey coexistence state E_{np}. Third, for even higher values of hunting cooperation, E_{np} becomes unstable. That is, there is bistability between the prey-only state and the predator–prey oscillations. The following regimes assume disease persistence ($R_0 > 1$) but are analog to the cases just described.
2. For low values of α (to the left of the limit point curve), hunting cooperation is too weak and predators go extinct (E_{ni}).

3. For sufficiently large hunting cooperation, there is a strong Allee effect in predators and bistability between the prey-only state E_{ni} and the endemic coexistence state E_{npi}.
4. For large values of α (to the right of the Hopf bifurcation curve), endemic coexistence is cyclic. The system is still bistable, with the other attractor being E_{ni}.

In this paper, we are particularly interested in the bistable regime, where the system shows tipping behavior in the sense that predators either go extinct or survive at stable equilibrium. We shall focus on the endemic case and therefore consider the dynamical regime no. 3, which covers a large part of the parameter range shown in Fig. 2. However, the analysis so far has not given us any information about the Allee threshold. Therefore, we do not know anything about the critical extinction threshold for the predators. Is it very high such that predators would have a hard time to survive in the bistable case, or is the Allee threshold quite low such that survival chances in the bistable case would be much better? With this is mind we proceed in studying the basins of attraction and in particular the surface that allows to separate them in the phase space.

3. Separatrix surface

In this section, we present a numerical method for analyzing the phase space and approximating the separatrix between different basins of attraction. We motivate this method as to find the Allee threshold in the eco-epidemiological model introduced earlier.

In general, the trajectories of a dynamical system approach different equilibria depending on certain conditions imposed on the parameters and depending on particular initial states. Thus we can partition the state space into different regions, i.e. the basins of attraction of one of the multiple stable states. In the eco-epidemiological model, there can be up to two stable states, which is why there are two basins of attraction, one for each of them. By reconstructing the separatrix curve between the basins of attraction, it is possible to study the Allee threshold representing the critical value of the predator density indicating when the system approaches predator extinction or predator–prey coexistence.

To this end, we develop an algorithm and implement it in Matlab, based on two fundamental steps:

1. Detection of points lying on the surface.
2. Reconstruction of the separatrix using a Moving Least Squares (MLS) quasi-interpolant.

3.1. Detection of separatrix points

In [14] the authors present a method to determine separatrix points. They consider $N \times N$ points gridded on the faces of the cubic domain $[0, l]^3$. Then, if the solutions of the model converge to different attractors, they consider initial conditions in pairs and employ the bisection method. In the phase space (n, p, i), the following initial conditions are considered:

$$\begin{aligned} &(n_j, p_j, 0) \text{ and } (n_j, p_j, l), \quad j = 1, \dots, N^2, \\ &(n_j, 0, i_j) \text{ and } (n_j, l, i_j), \quad j = 1, \dots, N^2, \\ &(0, p_j, i_j) \text{ and } (l, p_j, i_j), \quad j = 1, \dots, N^2. \end{aligned}$$

Fig. 3A shows an example of different trajectories starting from various initial conditions in the phase space. Fixing the biological parameters and starting from different initial conditions (red circles), the populations reach one of the two different stable equilibria (green stars). When looking at the diagram, we already get an idea about the location of the separatrix surface in the phase space. In particular, when projecting the phase space on the plane (n, p) (Fig. 3B), we note that the long term evolution of the trajectories depends mainly on predator densities. In fact, the previous Section has shown the existence of a strong Allee effect in predators linked with the bistability. If the predator density is below the Allee threshold, predators go extinct and otherwise they persist, reaching the coexistence equilibrium E_{npi}. From these observations we can state that the separatrix surface is located between the planes $\pi_1 : p = 0$ and $\pi_2 : p = l$. Hence, the set of the initial conditions reduces to:

$$P_{1j} = (n_j, 0, i_j), \quad P_{2j} = (n_j, l, i_j), \quad j = 1, \dots, N^2. \tag{5}$$

Therefore, we integrate model (1)–(3) on the cubic domain $[0, 1]^3$ by considering $N = 8$ equispaced points on each the n-axis and the i-axis. By applying the bisection method to the 64 pairs of initial conditions we obtain the scattered points of the separatrix shown in Fig. 4.

3.2. Approximation of the surface

In order to reconstruct the separatrix surface, we connect the scattered points found in the previous subsection by means of a Moving Least Squares approximation (MLS) belonging to the class of mesh-less numerical method, that have been employed in many areas of science [1,2,19]. The main idea of the MLS it is to approximate a function f, on the evaluation points $\mathbf{y} \in \mathbb{R}^d$, by solving small weighted least squares problems.

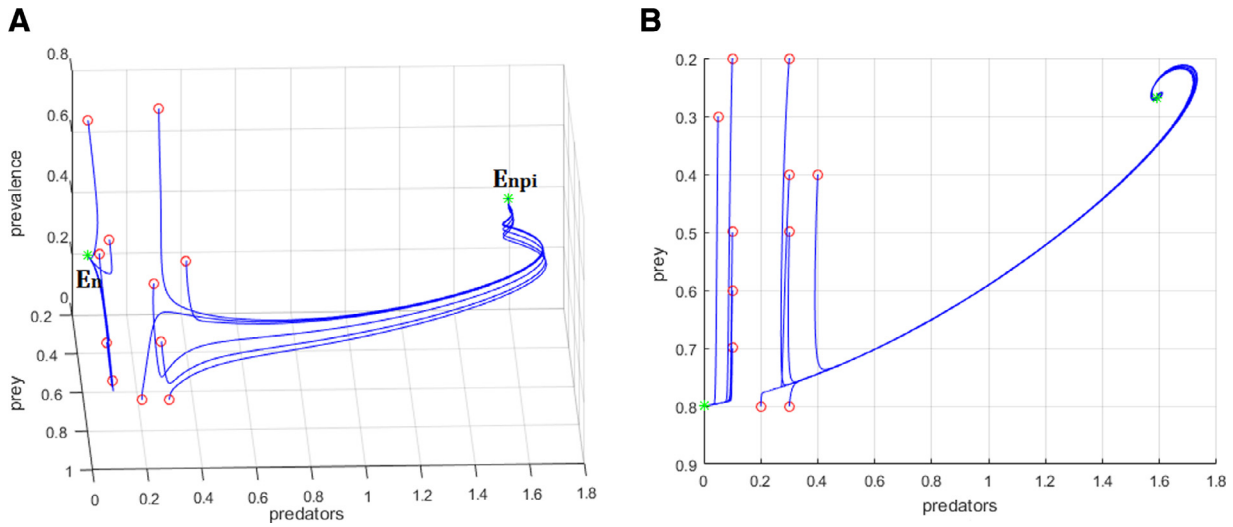

Fig. 3. Example of trajectories of model (1)–(3) starting from different initial conditions represented by the red empty circles and approaching equilibrium points (green stars) in 3D phase space (A) and projected on the phase plane (n, p) (B). Parameter values: $\alpha = 2$, $\beta = 2$, and the other ones as in Fig. 1. (For interpretation of the references to color in this figure legend, the reader is referred to the web version of this article.)

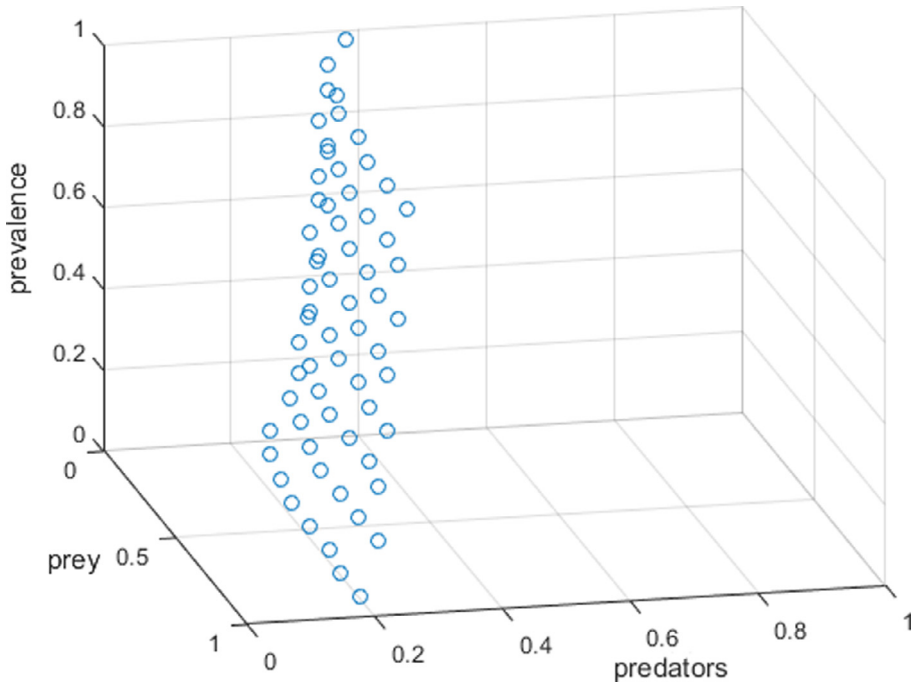

Fig. 4. Scattered separatrix points. Parameter values as in Fig. 3.

Given a discrete set $\chi = \{\mathbf{x}_1, \ldots, \mathbf{x}_N\} \subset \mathbb{R}^d$ of data sites and knowing the evaluation of the function f at these points: $\{f(\mathbf{x}_1), ..., f(\mathbf{x}_N)\}$, following the Backus–Gilbert approach [4,18], we construct the quasi-interpolant:

$$P_f(\mathbf{y}) = \sum_{i=1}^{N} f(\mathbf{x}_i)\Phi_i(\mathbf{y}), \tag{6}$$

where $\Phi_i(\mathbf{y}) = \Phi(\mathbf{y}, \mathbf{x}_i)$ are the *generating functions* that govern the approximation goodness. For each evaluation point the aim is to find the functions Φ_i minimizing the quantity

$$\frac{1}{2}\sum_{i=1}^{N} \Phi_i^2(\mathbf{y})\frac{1}{\omega(\mathbf{x}_i, \mathbf{y})}, \tag{7}$$

where ω is the weight function governing the data influence and becomes smaller the further away from each other its arguments are. Specifically, we used a compactly supported radial basis function

$$\forall \mathbf{x}, \mathbf{y} \in \mathbb{R}^d \quad \omega_\epsilon(\mathbf{x}, \mathbf{y}) = 0 \ if \ ||\mathbf{x} - \mathbf{y}||_2 > \epsilon, \tag{8}$$

where ϵ is the so-called *shape parameter* which influences the approximation goodness [40].

In order to ensure that the quasi-interpolant P_f achieves a certain approximation power, it is required that the generating functions Φ_i, reproduce polynomials of a certain degree q. Thus they are subject to the constraints

$$\sum_{i=1}^{N} p(\mathbf{x}_i)\Phi_i(\mathbf{y}) = p(\mathbf{y}) \quad \forall p \in \mathbf{\Pi}_q^d, \tag{9}$$

where $\mathbf{\Pi}_q^d$ is the space of the d-variate polynomials of total degree at most q with dimension $Q = \frac{(d+q)!}{q!d!}$.

By considering the vector $\Phi(\mathbf{y}) = [\Phi_1(\mathbf{y}), \ldots, \Phi_N(\mathbf{y})]$ we can rewrite (7) in matrix form:

$$\frac{1}{2}\mathbf{\Phi}^T(\mathbf{y})\mathbf{W}(\mathbf{y})\mathbf{\Phi}(\mathbf{y}), \quad \text{with} \quad \mathbf{W}(\mathbf{y}) = diag\Big(\frac{1}{\omega(\mathbf{x}_1, \mathbf{y})}, \ldots, \frac{1}{\omega(\mathbf{x}_N, \mathbf{y})}\Big), \tag{10}$$

and the linear polynomial constraint (9) becomes:

$$\mathbf{A\Phi}(\mathbf{y}) = \mathbf{p}(\mathbf{y}) \tag{11}$$

with $A_{ki} = p_k(\mathbf{x}_i),\ k = 1, \ldots, Q,\ i = 1, \ldots, N$ being the entries of matrix A and $\mathbf{p} = [p_1(\mathbf{y}), \ldots, p_Q(\mathbf{y})]^T$ being the known vector. The generating functions Φ satisfying (10) and (11) are given by:

$$\Phi_i(\mathbf{y}) = \omega(\mathbf{x}_i, \mathbf{y}) \sum_{k=1}^{Q} \lambda_k p_k(\mathbf{x}_i) \quad i = 1, \ldots, N, \tag{12}$$

where λ_k are the Lagrange multipliers, i.e. the only solutions of the system

$$\sum_{k=1}^{Q} \lambda_k \sum_{i=1}^{N} \omega(\mathbf{x}_i, \mathbf{y}) p_k(\mathbf{x}_i) p_q(\mathbf{x}_i) = p_q(\mathbf{y}) \quad 0 \le q \le Q. \tag{13}$$

Therefore, by considering the vector $\Lambda = [\lambda_1, \ldots, \lambda_N]$, and by letting $K(\mathbf{x}_i, \mathbf{y}) = \omega(\mathbf{x}_i, \mathbf{x})\Lambda^T(\mathbf{x})p(\mathbf{x}_i)$, the quasi-interpolant is:

$$P_f(\mathbf{y}) = \sum_{i=1}^{N} f(\mathbf{x}_i) K(\mathbf{x}_i, \mathbf{y}). \tag{14}$$

In order to improve the stability of the method, the polynomials are centered on the evaluation points, i.e. $p(\mathbf{x}_i) = p(\mathbf{y} - \mathbf{x}_i)$ so that only $p_1(\mathbf{y}) \equiv 1 \neq 0$ [18,40].

Constructing the quasi-interpolant (14), most of the computational cost is for the estimation of Lagrange multipliers λ_k, requiring the solution of system (13) for each evaluation point $\mathbf{y}$. This appears to be quite expensive, but there are two important factors to consider.

First, for our purpose, to reconstruct the surface we do not need a large number of evaluation points. Second, the linear polynomial reproduction ($q = 1$) is proved to be of approximation order $O(h^2)$ [18], and it is accurate enough in our contest. Since we are in $\mathbb{R}^2$, the linear system (13) that we have to solve is:

$$G(\mathbf{y})\lambda(\mathbf{y}) = p(\mathbf{y}), \quad \mathbf{y} \in \mathbb{R}^2, \tag{15}$$

where G is the Gram matrix with entries $G_{jk}(\mathbf{y}) = \sum_{i=1}^{N} p_k(\mathbf{x}_i) p_l(\mathbf{x}_i)\omega(\mathbf{x}_i, \mathbf{y})$ and $j, k = 1, \ldots, 3$.

Thanks to the low dimension of the problem in the computation we use Maple to find the explicit formula for the Lagrange multipliers:

$$\lambda_1(\mathbf{y}) = \frac{1}{|G|}(G_{11}^2 - G_{22}G_{33}),$$

$$\lambda_2(\mathbf{y}) = \frac{1}{|G|}(G_{12}G_{31} - G_{13}G_{23}),$$

$$\lambda_3(\mathbf{y}) = \frac{1}{D}(G_{22}G_{13} - G_{13}G_{23}).$$

In this way the solution of the linear system is avoided at all and for each evaluation point $\mathbf{y}$ the computational cost is at most

$$O(Q^3 + Q^2 N_y + Q N_y), \tag{16}$$

where N_y is the number of data sites inside the support of the weighted functions $w(\cdot, y)$ [40].

We are now ready to construct the separatrix manifold. We assume the data sites χ as the scattered points projected onto the (n, p) plane, while the data values $f_i = f(\mathbf{x}_i)$ describe the height at $\mathbf{x}_i$. Then we apply the MLS method just described in generating the local approximation.

The sketch of the overall algorithm is shown in Fig. 5. In the next section we provide some numerical results by using the Matlab software.

Step 1 Define the grid points P_{ij}
$i = 1,2\,;\ j = 1, \ldots N^2$

Step 2 Repeat *for* $j = 1, \ldots N^2$

2.1 *If* $P_{1j} \equiv (0,0,0)$ *or* $P_{2j} \equiv (0,0,0)$ *then return*
else

2.2 *If* $P_{1j} \to E_{ni}$ *and* $P_{2j} \to E_{npi}$ *or vice versa*
then $Separatrixpoints = Bisection(P_{1j}, P_{2j})$

Step 3 Define the evaluation points $\boldsymbol{y}$ and the weight functions $\boldsymbol{\omega}$

Step 4 Calculate the vector of the Lagrange Multipliers:
$\boldsymbol{\lambda} = LagrangeMultipliers(\boldsymbol{y}, Separatrixpoints, \boldsymbol{\omega})$

Step 5 Find the MLS approximant:
$\boldsymbol{P_f} = MLS(\boldsymbol{\lambda}, \boldsymbol{y}, Separatrixpoints, \boldsymbol{\omega})$

Fig. 5. Pseudo-code of the algorithm to detect and to connect the separatrix points.

4. Numerical experiments

In this section, we apply the method to reconstruct the separatrix surface in the eco-epidemiological model. The aim is to approximate the Allee thresholds in the bistable regime which correspond to the predator population densities necessary for survival. For the numerical experiments we use model (1)–(3) with the biological parameter values $r = 10$, $k = 0.8$, $m = 0.3$, $\theta = 0.1$ and integrate over one side of the cubic domain of the 3D phase space, [0, 1]. We take $N = 8$ equispaced points on both the n-axis and the i-axis as starting conditions for the bisection method to obtain a sufficient number of separatrix points. We iterate the method until the tolerance 10^{-4} is obtained. We choose the Wendland C2 compactly supported function, centered on $\mathbf{y}$, as weights:

$$\omega(\mathbf{x}_i, \mathbf{y}) = (1 - \epsilon||\mathbf{y} - \mathbf{x}_i||_2)_+^4 (4\epsilon||\mathbf{y} - \mathbf{x}_i||_2 + 1). \tag{17}$$

For our model a good approximation is found empirically with the shape parameter $1 \le \epsilon \le 3$, and our numerical studies use $\epsilon = 1.5$. In the following, we present the analysis of the basins of attraction of the prey-only equilibrium E_{ni} and coexistence equilibrium E_{npi} by varying the hunting cooperation α and disease transmissibility β.

Fig. 6A shows the separatrix for a given set of parameters. We observe that whether the system approaches the prey-only state or the coexistence state depends mainly on the predator density, in particular its relative size to the Allee threshold. The Allee threshold varies as a function of both disease prevalence and prey density. If disease prevalence is higher, the Allee threshold tends to increase as well. This seems plausible, as pack hunting requires more predators to compensate for disease-related mortality. If prey density is higher, the Allee threshold tends to decrease. This seems plausible as well, because less pack hunting is needed in the presence of more resources for the predators.

Fig. 6B shows the separatrix for increased disease transmissibility. As a consequence, there will be more infections (see the increased prevalences of the stationary states) and correspondingly higher disease-related mortality rates, which need to be compensated by pack hunting for the predators to survive. Therefore, the Allee thresholds tend to be larger, which is why the separatrix has shifted to the right-hand side (i.e., in the positive predator direction) in comparison to Fig. 6A.

We now consider the interesting case of varying hunting cooperation, α (Fig. 7). If hunting cooperation increases, the separatrix surface moves closer to the plane $p = 0$, considerably reducing the basin of attraction of the prey-only state E_{ni} (compare Fig. 7B with Fig. 7A). Therefore, the trajectories of the system almost always tend to the coexistence state E_{npi} except for very low predator densities.

So far we have seen that disease transmissibility tends to increase the Allee threshold, whereas hunting cooperation tends to decrease the Allee threshold. If we increase the two parameters β and α simultaneously, we observe, for the parameter set chosen in Fig. 7C, that the separatrix surface moves close to the plane $p = 0$. This means that the impact of pack hunting prevails even when disease transmission increases. The location of the Allee thresholds thus complements the results from a bifurcation analysis [24].

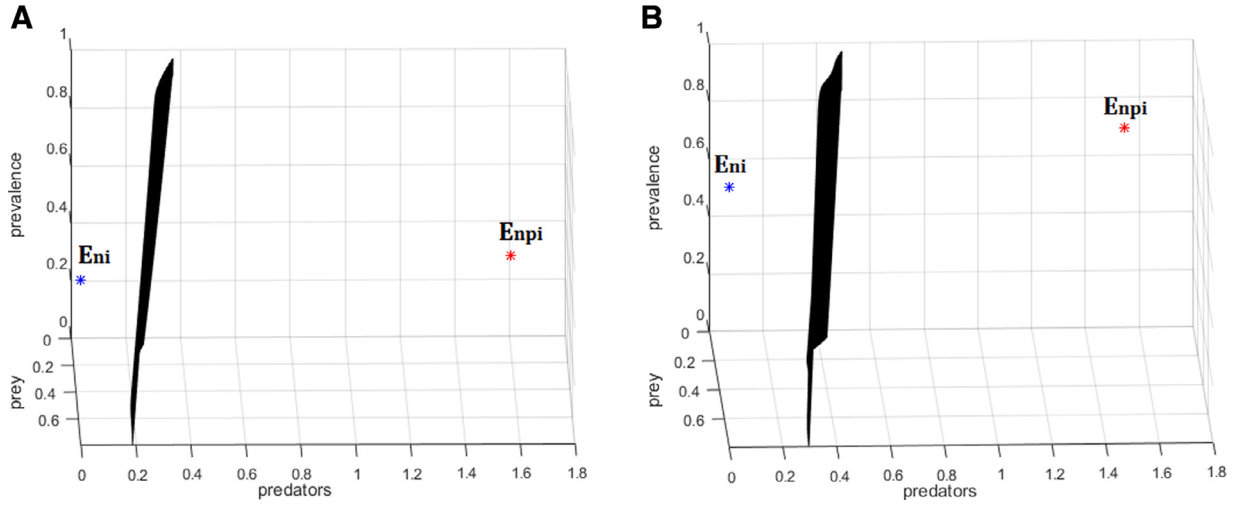

Fig. 6. Separatrix curve for different values of β. (A) $\alpha = 2$, $\beta = 2$; (B) $\alpha = 2$, $\beta = 8$. The blue star represents E_{ni} and the red one is E_{npi}. Other parameter values as in Fig. 1. (For interpretation of the references to color in this figure legend, the reader is referred to the web version of this article.)

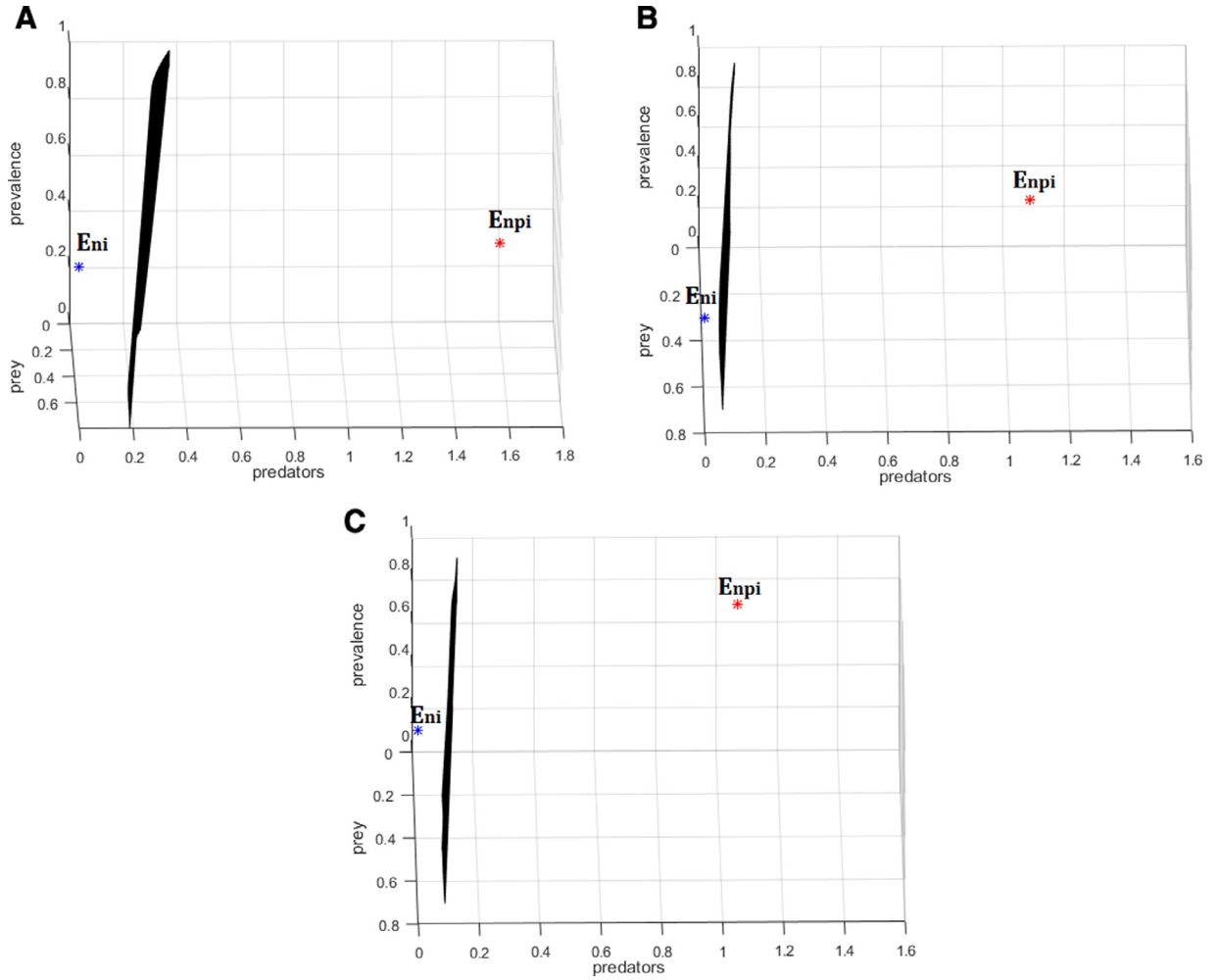

Fig. 7. Separatrix curve for different values of α and β. (A) $\alpha = 2$; $\beta = 2$, (B) $\alpha = 6$; $\beta = 2$ (C) $\alpha = 6$, $\beta = 8$. The blue star represents E_{ni} and the red one is E_{npi}. Other parameter values as in Fig. 1. (For interpretation of the references to color in this figure legend, the reader is referred to the web version of this article.)

Table 2
Execution times for the detection and the reconstruction of the separatrices by fixing different values of α and β.

Separatrix	Detection time	Reconstruction time
$\alpha = 2,\ \beta = 2$	2.50 min	35 s
$\alpha = 2,\ \beta = 8$	2.35 min	40 s
$\alpha = 6,\ \beta = 2$	2.27 min	47 s
$\alpha = 6,\ \beta = 8$	2.42 min	32 s

Table 2 reports the execution times to detect and to reconstruct the separatrices for different values of the parameters α and β.

5. Conclusions and future work

In this paper, we have presented a numerical tool to study the separatrix manifold of two basins of attraction. After detecting the separatrix points we reconnect them by means of the Moving Least Squares approximant. This method presents a number of advantages in the surface reconstruction, without the need of solving a linear system. We have to solve small weighted problems depending on the different evaluation points. In particular, working with bi- or tri-dimensional data sites, it is possible to find the explicit formula for the Lagrange multipliers.

For our case studies of the eco-epidemiological model (1)–(3), only a few evaluation points have been necessary. However, a larger number of evaluation points might require parallelization of the method.

The separatrix is the key in understanding and studying the Allee thresholds of the eco-epidemiological model. Standard equilibrium and stability analysis as well as bifurcation and continuation methods provide various insights, but do not give us information about the Allee threshold itself. Being the critical predator density needed for survival, this threshold is an important quantity, especially when it comes to population management. One may think of control programs to eradicate predators that are pests (e.g. in the case of biological invasions) or one may think of conservation programs where a sufficient number of reintroductions are needed to preserve an endangered predator population.

Moreover, the numerical method allows us to underline and to understand the impact of pack hunting and disease transmission directly on the Allee threshold. In particular, even if the bifurcation analysis presents bistability suggesting a strong Allee effect in the predator population, we have demonstrated that for large hunting cooperation the basin of attraction of the predator-extinction state contains only initial conditions with rather small predator densities. This might be interpreted in such a way that the Allee threshold is almost zero, in which case the predators almost always survive and are not very much affected by the stability. In other terms, pack hunting can not only mediate predator survival by inducing a strong Allee effect, but it can be so powerful that it turns a strong Allee effect effectively into a weak Allee effect. The difference is that in the latter case predator survival is (almost always) guaranteed, whereas in the former case an initial number of predators above the Allee threshold is needed for survival.

In future work we plan to further improve the method [21] by speeding up the detection of the separatrix points, using the theory of the stable manifold of the equilibrium points to reduce the integration domain.

Acknowledgments

The research has been partially supported by the projects “Metodi numerici in teoria delle popolazioni”, “Metodi numerici nelle scienze applicate” of the Dipartimento di Matematica “Giuseppe Peano” of the Università di Torino and by GNCS Project 2017 of the Istituto Nazionale di Alta Matematica – INDAM . The activity has been accomplished within the RITA “Research ITalian network on Approximation”.

References

[1] G. Ala, G.E. Fasshauer, E. Francomano, S. Ganci, M.J. McCourt, An augumented MFS approach for brain activity reconstruction, Math. Comput. Simul. (2017), doi:10.1016/j.matcom.2016.11.009. (in press).
[2] G. Ala, G.E. Fasshauer, E. Francomano, S. Ganci, M.J. McCourt, The method of fundamental solutions in solving Couled boundary value problems for M/EEG, SIAM J. Sci. Comput. 37 (4) (2015) B570–B590.
[3] W.C. Allee, Animal Aggregations. A Study in General Sociology, University of Chicago Press, Chicago, 1931.
[4] G. Backus, F. Gilbert, The resolving power of gross Earth data, Geophys. J. R. Astr. Soc. 16 (1968) 169–205.
[5] A.M. Bate, F.M. Hilker, Disease in group-defending prey can benefit predators, Theor. Ecol. 7 (2014) 87–110.
[6] B.E. Beisner, D.T. Haydon, K. Cuddington, Alternative stable states in ecology, Front. Ecol. Environ. 1 (2003) 376–382.
[7] L. Berec, D.S. Boukal, M. Berec, Linking the Allee effect, sexual reproduction, and temperature-dependent sex determination via spatial dynamics, Am. Nat. 157 (2001) 217–230.
[8] L. Berec, D.S. Boukal, Implications of mate search, mate choice and divorce rate for population dynamics of sexually reproducing species, Oikos 104 (2004) 122–132.
[9] D.D. Briske, S.D. Fuhlendorf, F.E. Smeins, A unified framework for assessment and application of ecological thresholds, Rangel. Ecol. Manag. 59 (2006) 225–236.
[10] S.R. Carpenter, D. Ludwig, W.A. Brock, Management of eutrophication for lakes subject to potentially irreversible change, Ecol. Appl. 9 (1999) 751–771.
[11] R. Cavoretto, S. De Marchi, A. De Rossi, E. Perracchione, G. Santin, Approximating basins of attraction for dynamical systems via stable radial bases, AIP Conf. Proc. 1738 (2016) 390003-1–390003-4.

[12] R. Cavoretto, A. De Rossi, E. Perracchione, E. Venturino, Graphical representation of separatrices of attraction basins in two and three-dimensional dynamical systems, Int. J. Comput. Methods 14 (2017) 1750008-1–1750008-16.
[13] R. Cavoretto, A. De Rossi, E. Perracchione, E. Venturino, Robust approximation algorithms for the detection of attraction basins in dynamical systems, J. Sci. Comput. 68 (2016) 395–415.
[14] R. Cavoretto, A. De Rossi, E. Perracchione, E. Venturino, Reliable approximation of separatrix manifolds in competition models with safety niches, Int. J. Comput. Math. 92 (2015) 1826–1837.
[15] F. Courchamp, L. Berec, J. Gascoigne, Allee Effects in Ecology and Conservation, Oxford University Press, New York, 2008.
[16] F. Courchamp, D.W. Macdonald, Crucial importance of pack size in the african wild dog, Lycaon pictus, Anim. Conserv. 4 (2001) 169–174.
[17] S. Creel, N.M. Creel, Communal hunting and pack size in african wild dogs, Anim. Behav. 50 (1995) 1325–1339.
[18] G.E. Fassahuer, in: Meshfree approximation methods with MATLAB, World Scientific Publishing Co., Singapore, 2007.
[19] G. Ala, E. Francomano, G.E. Fasshauer, S. Ganci, M.J. McCourt, A meshfree solver for the MEG forward problem, IEEE Trans. Magn. 51 (3) (2015). 5000304
[20] E. Francomano, F.M. Hilker, M. Paliaga, E. Venturino, On basins of attraction for a predator-prey model via meshless approximation, AIP Conf. Proc. 1776 (2016). 070007-1,070007-4.
[21] E. Francomano, F.M. Hilker, M. Paliaga, E. Venturino, An efficient method to reconstruct invariant manifolds of saddle points, Dolomites Research Notes on Approximation 10 (2017) 25–30.
[22] G. Gimmelli, B.W. Kooi, E. Venturino, Ecoepidemic models with prey group defense and feeding saturation, Ecol. Complex. 22 (2015) 50–58.
[23] P.M. Groffman, J.S. Baron, T. Blett, A.J. Gold, I. Goodman, L.H. Gunderson, B.M. Levinson, M.A. Palmer, H.W. Paerl, G.D. Peterson, N.L. Poff, D.W. Rejeski, J.F. Reynolds, M.G. Turner, K.C. Weathers, J. Wien, Ecological thresholds: the key to successful environmental management or an important concept with no practical application? Ecosystems 9 (2006) 1–13.
[24] F.M. Hilker, M. Paliaga, E. Venturino, Mathematical modeling of disease spread among cooperating predators, Bull. Math. Biol. (2017), doi:10.1007/s11538-017-0325-y.
[25] C.S. Holling, Resilience and stability of ecological systems, Ann. Rev. Ecol. Syst. 4 (1973) 1–23.
[26] G.R. Joldesa, H.A. Chowdhurya, A. Witteka, B. Doylea, K. Millera, Modified moving least squares with polynomial bases for scattered data approximation, Appl. Math. Comput. 266 (2015) 893–902.
[27] R.C. Lewontin, The meaning of stability, Brookhaven Symp. Biol. 22 (1969) 13–24.
[28] R.M. May, Thresholds and breakpoints in ecosystems with a multiplicity of stable states, Nature 269 (1977) 471–477.
[29] T.A. McMahon, R.M. Vogel, M.C. Peel, G.S. Pegram, Global streamflows: characteristics of annual streamflows, J. Hydrol. 347 (2007) 243–259.
[30] P.J. Mumby, A. Hastings, H.J. Edwards, Thresholds and the resilience of Caribbean coral reefs, Nature 450 (2007) 98–101.
[31] J.D. Murray, Mathematical Biology I: An Introduction, third ed., Springer, New York, 2002.
[32] R.M. Peterman, A simple mechanism that causes collapsing stability regions in exploited salmonid populations, J. Fish. Res. Board Can. 34 (1977) 1130–1142.
[33] P. Petraitis, Multiple Stable States in Natural Ecosystems, Oxford University Press, Oxford, 2013.
[34] Z. Ratajczak, J.B. Nippert, T.W. Ocheltree, Abrupt transition of mesic grassland to shrubland: evidence for thresholds, alternative attractors, and regime shifts, Ecology 95 (2004) 2633–2645.
[35] D.R. Rubenstein, I.J. Lovette, Temporal environmental variability drives the evolution of cooperative breeding in birds, Curr. Biol. 17 (16) (2007) 1414–1419.
[36] M. Scheffer, Critical Transitions in Nature and Society, Princeton University Press, Princeton, 2009.
[37] P.E. Stander, Cooperative hunting in lions: role of individual, Behav. Ecol. Sociobiol. 29 (6) (1992) 445–454.
[38] J.P. Sutherland, Multiple stable points in natural communities, Am. Nat. 108 (1974) 859–873.
[39] M. Teixeira Alves, F.M. Hilker, Hunting cooperation and Allee effects in predators, J. Theor. Biol. 419 (2017) 13–22.
[40] H. Wendland, Scattered Data Approximation, Cambridge University Press, Cambridge, 2010.